Polar Meteorol. Glaciol., **15**, 43-54, 2001

Density, stratigraphy and accumulation at DT001 in Princess Elizabeth Land, East Antarctic Ice Sheet

Jiahong Wen[1,2], Jiancheng Kang[1], Dali Wang[1], Bo Sun[1], Yuansheng Li[1], Zhongqin Li[2] and Jun Li[3]

[1] *Polar Research Institute of China, Shanghai 200129, China*
[2] *Laboratory of Ice Core and Cold Regions Environment, CAREERI, CAS, Lanzhou 730000, China*
[3] *Antarctic CRC and Australian Antarctic Division, Hobart 7001, Australia*

Abstract: Density data and the stratigraphy profile from a 50 m firn core and a snow-pit at DT001 in Princess Elizabeth Land, East Antarctic Ice Sheet, show that the densification process there is of the cold densification process type. The depth of the first critical density is 10.4 m; the depth of the second critical density is assumed to be 60.4 m. There are only a few embryo depth hoar layers with thickness of several centimeters, and most of them overlie or underlie ice crusts. The relative light transmission variation of the firn core is not clear above 16.0 m; below that, the cyclic light transmission becomes obvious with increase of depth. There are relatively abundant ice crusts with an average of 7 crusts per meter in the firn core. It is concluded from the firn core dating by stratigraphy, $\delta^{18}O$ and chemical profiles, that the accumulation trend increased slightly over the last 250 years. The mean accumulation rate of the whole firn core is 130.7 mm of water equivalent per year.

1. Introduction

Density and stratigraphic profiles, as fundamental data in snow-ice research, are used to help determine the boundaries of annual accumulation layers and estimate annual accumulation rate. They are also used to reconstruct climate and environmental records which are documented in the ice sheet.

During the First Chinese Antarctic Inland Expedition in January 1997, two 50 m ice cores were drilled while some glaciological investigations were conducted at DT001 (71°11′11″S, 77°21′5″E, 2320 m a.s.l.) in Princess Elizabeth Land, East Antarctic Ice Sheet (Kang and Wang, 1997). The two boreholes were only about 0.5 m apart. The ice cores consist of firn since they do not reach the pore closing depth (Li *et al.*, 1999). Firn density measurement and detailed stratigraphic profile description in transmitted light were conducted on one of the two firn cores. Based on the work above, the characteristics of firn density and stratigraphic profile were analyzed. Firn core dating and accumulation rate were obtained from the stratigraphy, and chemical and $\delta^{18}O$ profiles in this paper.

2. Density-depth profile

To maintain the ice core integrity and prevent pollution, we did not cut the firn core

when collecting the density data. The density measurement method is to use a vernier caliper to measure length and diameter, and electric balance to weigh every section of the ice core. This method has been used previously and it has been shown that the data can reflect the general trend of density variation with depth though it will cover up subtle changes (Alley, 1980; Han *et al.*, 1994). The ice core has high quality with 6.48 cm mean diameter (minimum 6.31 cm, maximum 6.60 cm) and 27.30 cm mean length of density measurement samples (sections). There are 182 samples in the 50 m ice core.

2.1. Characteristics of density-depth profile

The densification processes in the shallow layer of the Antarctic ice sheet can be classified into 3 types, *i.e.*, warm, cold and alternate densification process types (Qin, 1987). The cold densification process type is distributed widely over the inland region of the ice sheet where the annual mean temperature is below $-25^{\circ}C$ (Qin, 1987). Compression and sintering are the dominant factors in the cold densification process, and no or little melt water participates in the whole process. Therefore, this cold densification type is located in the dry-snow zone in terms of ice formation. The annual mean temperature within the dry-snow zone is also below $-25^{\circ}C$ (Qin, 1988).

An automatic weather station was set up at station LGB59, 180 km distance (200 m higher) from DT001. The average temperature at LGB59 is $-35.2^{\circ}C$, calculated from the annual mean air temperature and 10 m firn temperature recovered by the automatic weather station, and 10 m firn temperature collected by traverse (Allison, 1998). The surface lapse rate is $1.0^{\circ}C/100$ m, calculated from the annual mean temperature difference between DT001 and Zhongshan Station (J. Kang and W. Wang, 1997, unpublished data). Thus, the annual mean temperature of $-33.0^{\circ}C$ at DT001 can be obtained. The elevation where annual mean temperature is $-25.0^{\circ}C$ is about 1520 m above sea level, that is the height of lower limit of cold densification type, also the lower limit of dry-snow zone or the dry-snow line. DT001 is 800 m higher than the dry-snow line, so the densification process there belongs to the cold densification process type. The stratigraphic profile shows that, though the whole profile consists of abundant thin ice crusts, the formation of these ice crusts is mainly due to solar radiation and wind. The stratigraphic profile, without regelation ice layer, is remarkably simple in comparison with those in the coastal area (such as the northern side of Law Dome) or on the Antarctic Peninsula (Xie, 1985; Qin and Ren, 1991).

There exist two critical densities in the densification process from snow to ice: 550 kg m^{-3} and 830 kg m^{-3}, which are called the first critical density and the second critical density respectively (Maeno, 1982; Qin, 1995a). An inflexion around density 550 kg m^{-3} can be observed in the density-depth profile of DT001 firn core (Fig. 1a). The depth of the inflexion is between 10–11 m. A linear regression equation is produced from the data of density ρ (kg m^{-3}) and H (m) above 11 m depth: $\rho = 12.3H + 424.7$, $R^2 = 0.718$. The first critical depth at DT001, calculated from this equation, is 10.4 m. The depth is close to the critical depth of 11.5 m at W'200 on the Mizuho Plateau (Nishimura *et al.*, 1983). The elevation of 2000 m and annual mean temperature of $-33.1^{\circ}C$ at W'200 are also well-matched with those at DT001. Another regression equation can be obtained from the data of density ρ and H below 10 m depth: $\rho = 5.7H + 485.7$, $R^2 = 0.955$. The second critical depth, calculated from this equation, is 60.4 m. This depth

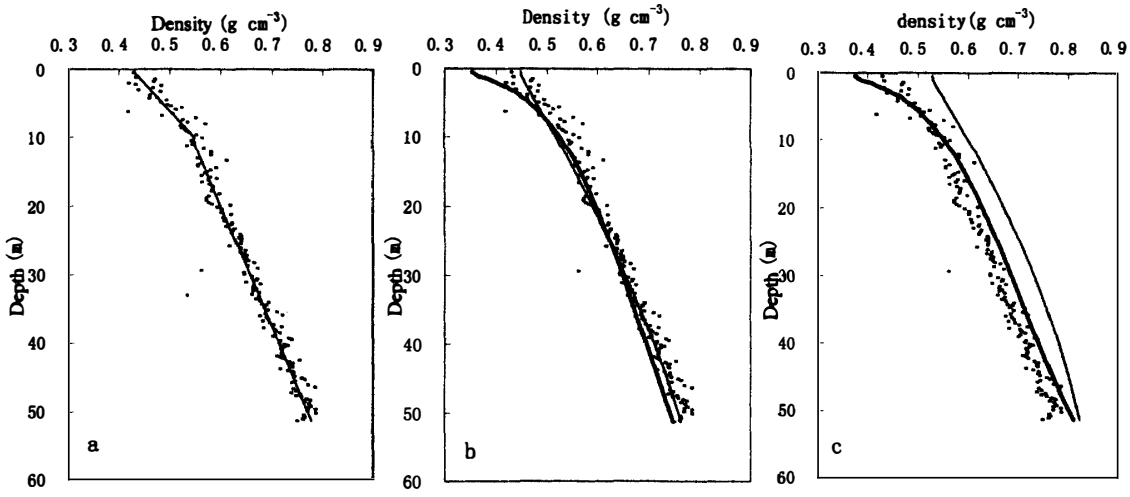

Fig. 1. Density-depth profiles for DT001 firn core (a). Results of model predictions by Kameda et al. (eq. (3), thick line; eq. (5), thin line) (b), and by Craven and Allison (eq. (6), thick line; eq. (7), thin line) (c).

corresponds to the pore closing depths at places with similar temperature and precipitation, such as Byrd station in Antarctica, and Inge Lehmann and Crête in Greenland (Gow, 1968, 1975; Paterson, 1981).

2.2. *Application of empirical models*

The densification process from snow to ice has been studied previously via both a theoretical viewpoint and empirical modeling. Schytt (1958) first established a relation between the firn density and the accumulated pressure of overlying snow layers. With glaciological investigations being conducted widely in polar regions and fundamental data (density and meteorological data) increasing continually, glaciologists who do empirical modeling have made marked progress in recent years. Langway *et al.* (1993) found a simple relation of overburden pressure with density:

$$P=A\exp(B(\rho_i-\rho)^2), \tag{1}$$

where P is the overburden pressure in bars, ρ_i is the pure ice density (generally defined as 917 kg m^{-3} at -20°C). A and B are constant. The overbudden pressure P from the surface to depth H is given by $P=9.8\times10^{-5}\int_0^H \rho\,\mathrm{dh}$.

Actually eq. (1) can be changed into the proportional relation of the logarithm of the overburden pressure with the square of the porosity:

$$\ln P=C_1S^2+C_2, \tag{2}$$

where S, porosity, is expressed as $(\rho_i-\rho)/\rho_i$.

Kameda *et al.* (1994) investigated the coefficients in eq. (2) and found a dependence of coefficient C_2 on 10 m firn temperature. Equation (2) became:

$$\ln P=-12.9S^2-0.0251T+7.6, \tag{3}$$

where T is the temperature in K.

Another model, by Kameda *et al.* (1994), is equivalent to the original proposal by Schytt (1958), *i.e.*, the overburden pressure and the porosity have the following relation:

$$P = C_3 \ln S + C_4. \tag{4}$$

Kameda *et al.* (1994) analyzed the dependence of coefficient C_3 on the 10 m depth firn temperature, and obtained the empirical model:

$$P = (0.0326\,T - 10.6)\ \ln S - 1.82. \tag{5}$$

Recently Craven and Allison (1998) further examined the dependence of densification on mean annual wind speed W in m s^{-1} and mean annual surface accumulation rate A in m a^{-1}, and further developed the empirical models proposed by Kameda *et al.* (1994). Multiple regression analyses on C_2 and C_3 were performed while C_1 and C_4 were held fixed. These gave expanded versions of eqs. (3) and (5):

$$\ln P = -12.9S^2 - 0.0249\,T - 0.1083\,W + 1.5968A + 7.91, \tag{6}$$

$$P = (0.048\,T + 0.1067\,W - 3.1743A - 14.1)\ \ln S - 1.82. \tag{7}$$

Empirical models (3) and (5) by Kameda *et al.* (1994) are not applicable to density data from both the percolation zone, such as S18 in Mizuho Plateau, and the area with low accumulation rate and strong katabatic-wind regime where the strong wind greatly enhances grain-settling rates in the upper few meters of the snowpack, such as Mizuho Station and station LGB35 at the southern extremity of an Australian National Antarctic Research Expedition (ANARE) traverse line (Kameda *et al.*, 1994; Craven and Allison, 1998). Figure 1b shows that eqs. (3) and (5) are applicable to site DT 001, which reflects, to some extent, the fact that this site is not located in the region with strong katabatic-wind regime and low accumulation rate.

Equation (6) yields a good fit to data through the first stage of densification up to around 0.70–0.75 g cm^{-3}, while eq. (7) gives a much better fit to data at higher densities where values asymptote to the bubble-free density of pure ice (Craven and Allison, 1998). Analyses of chemical data and the $\delta^{18}O$ profile of another firn core from DT001 show that there are approximately 250 annual layers in the 50 m firn core (Li *et al.*, 1999; Zhang *et al.*, 1999). A mean annual accumulation rate of 122.3 mm was calculated using the density-depth data of the firn core analyzed in this paper. According to the data from automatic weather stations set up by Australia in Lambert Glacier Basin, the larger the surface slope, the higher the wind speed. The surface slope is up to 3.2 –5.2 m km^{-1} where mean annual wind speed is larger than 10 m s^{-1}. DT001 is situated in a short flatter section before a sharper descent towards the coast (between 2290–2415 m a.s.l.) (Higham and Craven, 1997). Provided that the wind speed at DT001 is consistent with those measured by automatic weather stations at the sites in Lambert Basin where gradients are smaller, W is about 7.5 m s^{-1} (Allison, 1998). Thus Fig. 1c can be drawn using predictions by eqs. (6) and (7). Figure 1c shows eq. (6) gives a much better fit to density data while eq. (7) overestimates true densities. This is consistent with Craven and Allison's conclusion stated above (Craven and Allison, 1998).

Since both eqs. (6) and (7) take mean annual surface accumulation rate A as a variable, we can try to estimate the annual accumulation rate A at DT001 via these two empirical models. P of 0.0506 MPa at the first critical depth is derived from the density-depth data. Thus A of 156.0 mm and 237.2 mm can be calculated by eqs. (6) and (7) respectively. A of 156 mm is possibly closer to the true value because eq. (6) gives a better fit to the density data. Another prediction is possibly larger than the true annual accumulation rate since eq. (7) overestimates the measured density data.

Herron and Langway (1980) proposed that the mean annual accumulation rate may be estimated from the slope C' of the second stage of densification and mean annual temperature:

$$A=(\frac{\rho_i K_I}{C'})^2 , \tag{8}$$

where K_I is an Arrhenius-type rate constant. The mean annual accumulation rate of the firn core, calculated from this equation, is 128.1 mm.

3. Characteristics of the stratigraphic profile

The main features observed in a firn core on a light table are grain size, depth hoar, variable light transmissivity, melt phenomena, and wind crusts (Shoji and Langway, 1989). Since DT001 is located on the East Antarctic Plateau, there only exist thin ice crusts in the firn layer including radiation crusts and wind crusts (Fig. 2).

3.1. Grain size

Firn can be divided into fine, medium and coarse firn or into more detailed types according to grain size (Qin, 1988, 1995b; Wen *et al.*, 1996). When analyzing stratigraphy and determining annual layer boundaries of firn cores from inland Antarctica, we have to observe stratigraphic profiles as carefully as possible, because of its monotone and low accumulation, to recover stratigraphic features to the greatest extent. Grain size variation with depth is one of an important feature in stratigraphy. In this study, for the purpose of observing grain size variation in as much detail as possible, we classify the grain size into 13 types on the basis of the ratios of fine, medium and coarse firn (see Table 1). Furthermore, finer and coarser variations of grain size with depth are also marked according to its relative change within a type.

The grain size observation shows that the grain size variation with depth in DT001 stratigraphy can be divided into four sections: 1) from the surface to 7.76 m, the whole firn core consists of fine firn. Grain size ranges from 0.2–0.3 mm at the surface to about 0.7–0.8 mm near the section bottom, only some thin layers are slightly coarser than upper or lower adjacent strata. Grain size in the overall section is less than 1 mm. 2) 7.76–18.35 m, grain size fluctuates greatly between fine firn and medium firn with high frequency, in which some cyclic variations are discernible. 3) 18.35–41.19 m, main grain size types are medium firn, medium firn with a little coarse firn. In 29.68–33.45 m of this section, firn is coarser, most of this part consists of the type of medium firn with coarse firn, and some even consists of coarse firn with medium firn. Grain size in this

Table 1. The types of grain size.

No	Grain size types	Ratios
1	Fine firn	100% fine firn
2	Fine firn with a little medium firn	Fine firn more than 80%; medium firn less than 20%
3	Fine firn with medium firn	Fine firn more than 60%, less than 80%; medium firn more than 20%, less than 40%
4	Fine and medium firn in half-and-half	Fine firn more than 40%, less than 60%; medium firn more than 40%, less than 60%
5	Medium firn with fine firn	Fine firn more than 20%, less than 40%; medium firn more than 60%, less than 80%
6	Medium firn with a little fine firn	Fine firn less than 20%; medium firn more than 80%
7	Medium firn	100% medium firn
8	Medium firn with a little coarse firn	Medium firn more than 80%; coarse firn less than 20%
9	Medium firn with coarse firn	Medium firn more than 60%, less than 80%; coarse firn more than 20%, less than 40%
10	Medium and coarse firn in half-and-half	Medium firn more than 40%, less than 60%; coarse firn more than 40%, less than 60%
11	Coarse firn with medium firn	Medium firn more than 20%, less than 40%; coarse firn more than 60%, less than 80%
12	Coarse firn with a little medium firn	Medium firn less than 20%; coarse firn more than 80%
13	Coarse firn	100% coarse firn

section still varies frequently, but the variation range is not as large as that in the upper section. The grain size-depth profile mainly presents relatively coarser or finer rhythmic variation within a grain size type. 4) 41.19 m to the bottom of the firn core, it is difficult to distinguish the relative variation of grain size by the unaided eye. Only the slow transformation from one to another grain size type can be observed. Below 41.19 m, the firn core consists of coarse firn with a little medium firn.

In general, the grain size is coarser in summer layers, finer and more homogeneous in winter layers (Shoji and Langway, 1989). The variation of grain size, if the effect of depth hoar has been excluded, can reflect the variation of alternate seasons, and is a useful reference to determine annual boundaries. Grain sizes at some parts in the firn core are evidently coarser, which possibly indicate interannual climate changes.

3.2. Depth hoar

Depth hoar is not present in the snow-pit profile at DT001. Relatively coarser grain size (0.5–1.0 mm) occurs in 2.85–2.96 m in the firn core. Its structure, however, is not so loose as that of depth hoar, thus, it belongs to a summer layer rather than depth hoar. Again, down to 3.16–3.19 m and 3.66–3.70 m, firn is coarser and looser, and the transmissivity is slightly better. Two layers are depth hoar. There also exist a few similar strata in the firn core, which, in general, are only several centimeters thick, and usually overlie or underlie a thin ice crust. Until 7.76 m, grain size in the firn core belongs to the fine firn type (grain size less than 1.0 mm); thus, the depth hoar strata are

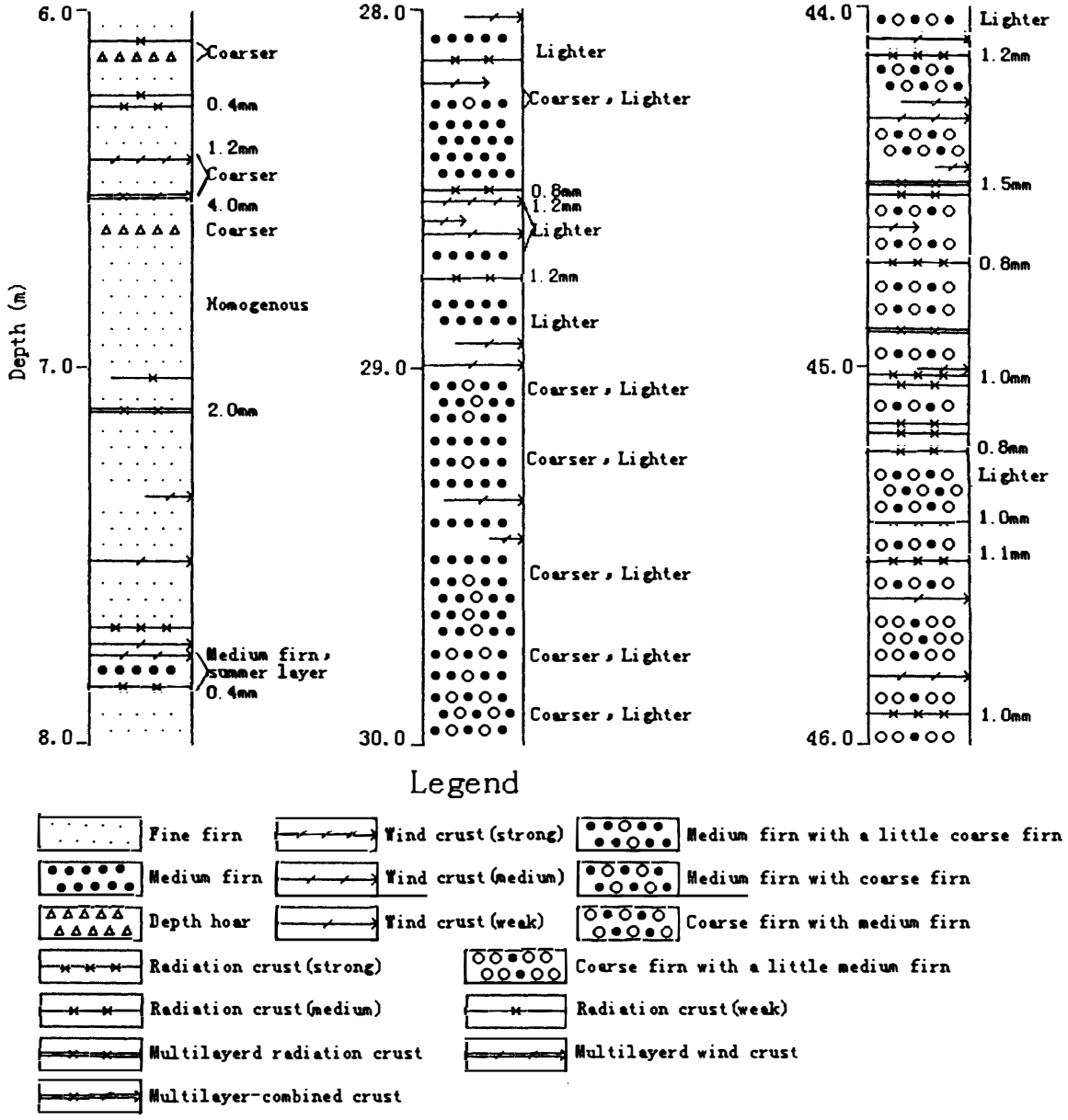

Fig. 2. Stratigraphic profiles of DT001 firn core from 6.0–8.0 m, 28.0–30.0 m and 44.0–46.0 m.

weak, which indicates that the depth hoar in this firn core does not develop well. Therefore, frequent variations of grain size under 7.76 m as stated above largely result from seasonal and interannual climate changes.

DT001, located in a short flatter section, is different from the sites where occurrence of depth hoar north of latitude 73°S are in more localized low accumulation sites, due to local topographic effects, such as the coastal slope with relatively strong katabatic winds (Higham and Craven, 1997). Therefore, the location of DT001 is not a suitable place for the development of depth hoar.

3.3. Light transmissivity

Shoji and Langway (1989) proposed that it is darker and multilayered in summer deposits and lighter and homogeneous in winter deposits by analyzing ice cores mainly from the Greenland Ice Sheet. We found, however, that summer deposits at DT001 lack multilayered structure due to lower annual accumulation and lack of melt layers. Moreover, it is lighter in summer deposits due to coarser grain size, lower density and more porosity. In contrast, it is denser, darker and homogeneous in winter deposits. Thus the light transmissivity in this firn core is different from that in Greenland ice cores. Relative variation of light transmissivity is not evident from surface to 16.0 m, below that, it becomes more and more clear, with cyclic variations that can be used for differentiating annual layers. In some sections, the boundaries of light transmissivity variation are clear enough that lighter and darker layer boundaries can be determined. But in other sections, since light transmissivity changes gradually, it is difficult to determine definite boundaries of light transmissivity variation; instead, we marked the positions of maximum and minimum lightness (Fig. 2).

3.4. Ice crusts

In general, thin ice crusts can be divided into three types: radiation crust, wind crust and mutilayered crust. In this paper, multilayered crust is further divided into three types: multilayered radiation crust, multilayered wind crust and multiplayer-combined crust (Fig. 2). Our observations on ice crusts include thickness, light transmissivity, single-layer or multilayer (adjacent ice crusts more than two layers), and clearness of the boundaries. Ice crusts are classified into strong, medium and weak types. Because the light transmissivity of radiation crusts is better, and the boundaries are clearer than those of wind crusts, two types can be distinguished. Transparent and semitransparent crusts are mainly formed in summer; therefore, they are an important reference to determine annual layer boundaries (Ren *et al.*, 1995).

There are a total of 351 ice crusts with an average of 7 crusts per meter in the 50 m firn core at DT001. Comparison with the result from Australian Lambert Glacier Basin traverses indicates that there are relatively abundant ice crusts at DT001. Their distributions with depth are 5.3 crusts per meter above 10 m, 7.2 crusts per meter between 10–20 m, 7.3 crusts per meter between 20–30 m, 4.9 crusts per meter between 30–40 m, 11.0 crusts per meter between 40–50 m. This shows that the distribution has no regularity, and also there does not exist a situation at GC46 in Wilkes Land in which almost all ice crusts occur in a shallow layer, below a certain depth, ice crusts disappear, possibly due to sublimation and condensation processes within the ice sheet (Qin, 1995a).

Two sections from 18.40–20.57 m and 29.34–32.38 m do not have ice crusts, except for a weak unpenetrated ice crust at 30.85 m, and grain sizes in both sections are slightly coarser. This presents a striking contrast to other sections where ice crusts occur frequently. The reason why it happens is still unknown.

4. Accumulation rate

There are abundant stratigraphic features in the DT001 firn core such as radiation crusts, grain size variation, light transmissivity and depth hoar texture, which show

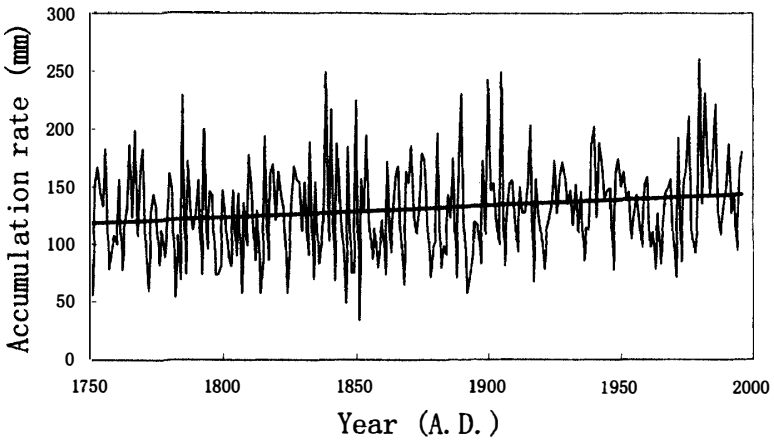

Fig. 3. Annual accumulation rate record of the firn core from 1749–1996.

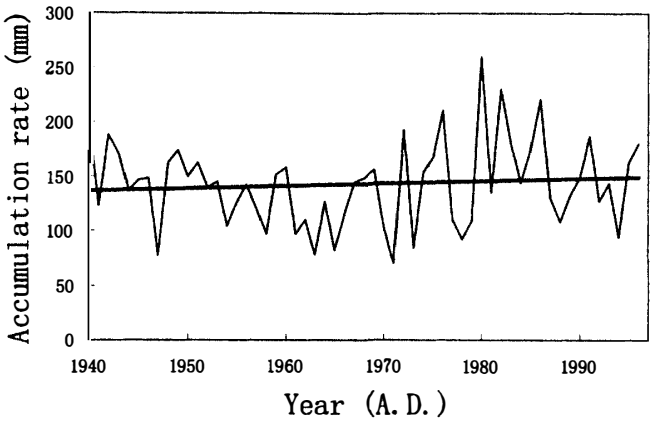

Fig. 4. Annual accumulation rate record of the firn core over the last 50 years.

seasonal variations. Meanwhile, Cl^-, Na^+, NO_3^- and $\delta^{18}O$ also present obvious seasonal signals. However, with the depth increasing, the seasonal signals of $\delta^{18}O$ are gradually smoothed below 3 m while the seasonal variations of Cl^-, Na^+ and NO_3^- persist in the whole firn core (Li *et al.*, 1999). Based on annual cycles of the stratigraphic features, chemical data and $\delta^{18}O$ profile, we determined the annual layer boundaries and obtained there are 246 annual layers from the surface to 51.28 m. The annual accumulation rate record from 1751 to 1996 is shown in Fig. 3. The mean annual value for the entire period is 130.7 mm. The accumulation rate has no large change except that its trend shows a slight increase over the last two and a half centuries.

Accumulation trend also presents an increase over the last 50 years. However, average accumulation rate of 116.3 mm in 1960's is lower than the mean value of the whole firn core (Fig. 4). Conversely, the snow accumulation has a decreasing trend in the last 50 years on another side (the west side) of Lambert Basin (Ren and Qin, 1998), reflecting complexity in temporary and spatial distribution of accumulation rate in this region.

The mean accumulation rate above the first critical depth, calculated by eq. (6), is 156.0 mm, while the mean value of the whole firn core, calculated from eq. (8), is 128.1

mm. In addition, the mean accumulation rate above the first critical depth and the mean value of the whole firn core, derived from stratigraphy, $\delta^{18}O$ and chemical profile, are 143.3 mm and 130.7 mm respectively. These indicate that the model results gave values similar to those derived by other methods.

5. Conclusions

The densification process and stratigraphic profile were discussed, and firn core dating was conducted in this paper. The major conclusions are as follows:

1) The firn densification process of snow/firn there is of the cold densification type. The depths of the first and second critical densities are 10.4 m and 60.4 m, respectively.

2) The depth hoar is not well developed. There are only a few embryo depth hoar layers with thickness of several centimeters; most of them overlie or underlie an ice crust.

3) According to fine, medium and coarse firn and their ratios, 13 grain-size types are classified from fine to coarse firn. The grain-size depth profile of the snow/firn layer at DT001 can be divided into four sections: 0–7.76 m, 7.76–18.35 m, 18.35–41.19 m, 41.19 m to the bottom of the firn core. Grain-size variations are mainly controlled by seasonal or interannual climate change.

4) The relative variation of light transmissivity of the firn core is not clear above 16.0 m, and then, gradually rhythmic light transmissivity occurs that can be considered as a reference for differentiating annual layers.

5) There are relatively abundant ice crusts with an average of 7 crusts per meter in the snow stratigraphic profile. However, two firn core sections with total length of 5.21 m only contain firn without ice crusts. Ice crust can mainly divided into three types: radiation crust, wind crust and multilayered crust. Multilayered crust can be further divided into three typesr: Multilayered radiation crust, multilayered wind crust and multilayer-combined crust. Radiation crust is of importance for determining annual layer boundaries.

6) The process of firnification at DT001 has been examined with two empirical models established by Craven and Allison (1998), Kameda *et al.* (1994). The results show that DT001 is not located in an area with strong katabatic winds and low accumulation rate.

7) The DT001 firn core is dated on the basis of various stratigraphic features, chemical data and $\delta^{18}O$ profile. It is concluded that accumulation shows a slight increase over the last 250 years. The mean accumulation rate of the whole profile is 130.7 mm a^{-1}. The accumulation rates derived from empirical models (eqs. (6) and (8)) are consistent with the result from stratigraphy, $\delta^{18}O$ and chemical profile.

Acknowledgments

This work was supported by the National Natural Science Foundation of China grant No. 49973006 and No. 40071022, Laboratory of Ice Core and Cold Regions Environment, Lanzhou Institute of Glaciology and Geocryology, CAS, and the Knowledge-Innovation Fund, CAS (KZCX2-303). Dr. Zhang Mingjun provided the

chemistry and oxygen isotope data for us. The NIPR provided support for two of us (Wen Jiahong and Li Yuansheng) to attend the symposium. Two anonymous reviewers gave valuable comments. Dr. Teruo Furukawa filled in as editor and gave helpful suggestions while executive editor Dr. Kumiko Goto-Azuma was working in the field. Members of the First Chinese Antarctic Inland Expedition assisted with acquiring the survey data and ice core drilling. The authors wish to thank all contributing persons and institutions.

Special thanks to executive editor Kumiko Goto-Azuma for her helpful suggestions and kind help.

References

Alley, R.B. (1980): Densification and recrystallization of firn at Dome C, East Antarctica. Inst. Polar Stud. Rep., **77**, 1–62.

Allison, I. (1998): Surface climate of the interior of the Lambert Glacier basin, Antarctica, from automatic weather station data. Ann. Glaciol., **27**, 515–520.

Benson, C.S. (1962): Stratigraphic studies in the snow and firn of the Greenland ice sheet. SIPRE Res. Rep., **70**, 1–35.

Craven, M. and Allison, I. (1998): Firnification and the effects of wind-packing on Antarctic snow. Ann. Glaciol., **27**, 239–245.

Han, J., Kang, J., Wen, J., Lluberas, A. and Rodriguez, F. (1994): General characteristics in stratigraphy and density variation for ice cores from Collins Ice Cap, King George Island, Antarctica. Antarct. Res. (Chinese Edition), **6** (**1**), 40–46 (in Chinese with English abstract).

Herron, M.M. and Langway, C.C., Jr. (1980): Firn densification: an empirical model. J. Glaciol., **25** (93), 373–385.

Higham, M. and Craven, M. (1997): Surface mass balance and snow surface properties from the Lambert Glacier Basin traverses 1990–1994. Antarct. CRC Rep., **9**, 1–45.

Gow, A.J. (1968): Deep cores studies of the accumulation and densification of snow at Byrd Station and Little America V, Antarctica. CRREL Res. Rep., **197**, 1–45.

Gow, A.J. (1975): Time-temperature dependence of sintering in perennial isothermal snowpacks. IAHS, **114**, 25–41.

Kang, J. and Wang, D. (1997): An investigation of 330 km glaciological profile from Zhongshan Station to inland of Antarctic Ice Sheet. Chinese J. Polar Res., **8** (2), 156–158.

Kameda, T., Shoji, H., Kawada, K., Watanabe, O. and Clausen, H.B. (1994): An empirical relation between overburden pressure and firn density. Ann. Glaciol., **20**, 87–94.

Langway, C.C., Jr., Shoji, H., Mitani, A. and Clausen, H.B. (1993): Transformation process observations of polar firn to ice. Ann. Glaciol., **18**, 199–202.

Li, Z., Zhang, M., Qin D., Xiao, C., Tian, L., Kang, J. and Li, J. (1999): Primary research on the seasonal variations of $\delta^{18}O$, Cl^-, NO_3^-, Na^+ and Ca^{2+} in the snow and firn recovered from Princess Elizabeth Land, Antarctica. Chinese Sci. Bull., **44** (24), 2270–2274.

Maeno, N. (1982): Densification rates of snow at polar glaciers. Mem. Natl Inst. Polar Res., Spec. Issue, **24**, 204-211.

Nishimura, H., Maeno, N. and Satow, K. (1983): Initial stage of densification of snow in Mizuho Plateau, Antarctica. Mem. Natl Inst. Polar Res., Spec. Issue, **39**, 149–158.

Paterson, W. S. B. (1981): The Physics of Glaciers, 2nd ed. Oxford, Pergamon Press, 380 p.

Qin, D. (1987): Densification process of snow firn in the surface layer of the Antarctic Ice Sheet. J. Glaciol. Geocryol., **9** (3), 190–204 (in Chinese with English abstract).

Qin, D. (1988): Research on the stratigraphy of shallow snow/firn core in Wilkes Land, Antarctica. The Collection of the Scientific Papers on the Antarctic Research (No.5) on the Glaciology. Beijing, Science Press, 22–59 (in Chinese with English abstract).

Qin, D. (1995a): Physical Process and Modern Climate and Environmental Record in the Surface Layer of the

Antarctic Ice Sheet. Beijing, Science Press, 32–59 (in Chinese).
Qin, D. (1995b): Report on Glaciological Research of the 1990 International Trans-Antarctic Expedition (1989–1994). Beijing, Science Press, 1–117.
Qin, D. and Ren, J. (1991): A preliminary study on the snow profile and surface characteristics of the 6000 km trans-Antarcitca. Sci. China (Ser. B), **21** (9), 963–969 (in Chinese).
Ren, J. and Qin, D. (1998): Distribution of stable isotopes in surface snow and climatic change in past decades over the Lambert Glacier Basin, East Antarctica. J. Glaciol. Geocryol., **20** (4), 425–431.
Ren, J., Qin, D., Allison, I., Higham, M. and Goodwin, I. (1995): A study of snow stratigraphy and accumulation-rate change in the west part of the Lambert Glacier Basin, East Antarctica. J. Glaciol. Geocryol., **17** (3), 247–281 (in Chinese with English abstract).
Schytt, V. (1958): Glaciology II. Snow Studies at Maudheim. Snow studies inland. The inner structure of the ice shelf at Maudheim as shown by core drilling. Norwegian-British-Swedish Antarctic Expedition, 1945–52. Sci. Results, **4 (2A)**, 1–64.
Shoji, H. and Langway, C.C., Jr. (1989): Physical property reference horizons. The Environmental Record in Glaciers and Ice Sheets, ed. by H. Oeschger and C.C. Langway, Jr. New York, J. Wiley, 161–176.
Wen, J., Kang, J., Han, J., Liu, L., Wang, D., Yan, M. and Li, Y. (1996): A preliminary research on the annual layer differentiation and mass balance of ice cores from Collins Ice Cap. Studies on the Interaction and Impact between Antarctic and Global Climate and Environment, ed. by X. Zhou and R. Lu. Beijing, Meteorology Press, 210–215 (in Chinese).
Xie, Z. (1985): Ice formation and ice structure on Law Dome, Antarctica. Ann. Glaciol., **6**, 150–153.
Zhang, M., Li, Z., Qin, D., Xia C., Kang, J. and Li, J. (1999): The study on the depositional styles of major ions and the climatic effect of $nssSO_4^{2-}$ in Princess Elizabeth Land, Antarctica. Chinese J. Polar Res., **11** (3), 161–168 (in Chinese with English abstract).

(Received January 4, 2001; Revised manuscript accepted July 2, 2001)